Bifunctional Aptamer Drug Carrier Enabling Selective and Efficient Incorporation of an Approved Anticancer Drug Irinotecan to Fibrin Gels

Hiroto Fujita, Yuka Kataoka and Masayasu Kuwahara * (ID)

Graduate School of Integrated Basic Sciences, Nihon University, 3-25-40 Sakurajosui, Setagaya-ku,
Tokyo 156-8550, Japan; fujita.hiroto@nihon-u.ac.jp (H.F.); kataoka.yuka@nihon-u.ac.jp (Y.K.)
* Correspondence: mkuwa@chs.nihon-u.ac.jp; Tel.: +81-03-5317-9398

check for
updates

Abstract: We have previously developed a bifunctional aptamer (bApt) binding to both human thrombin and camptothecin derivative (CPT1), and showed that bApt acts as a drug carrier under the phenomenon named selective oligonucleotide entrapment in fibrin polymers (SOEF), which enables efficient enrichment of CPT1 into fibrin gels, resulting in significant inhibition of tumor cell growth. However, although the derivative CPT1 exhibits anticancer activity, it is not an approved drug. In this study, we evaluated the binding properties of bApt to irinotecan, a camptothecin analog commonly used for anticancer drug therapy, in addition to unmodified camptothecin (CPT). Furthermore, we have revealed that irinotecan binds to bApt like CPT1 and is selectively concentrated on fibrin gels formed around the tumor cells under the SOEF phenomenon to suppress cell proliferation.

Keywords: drug delivery system; anticancer drug; camptothecin derivative; irinotecan

1. Introduction

Highly water-soluble derivatives of camptothecin, a type of quinoline alkaloid (irinotecan and topotecan), are currently known to have a broad spectrum of anticancer activity such as in lung cancer, colorectal cancer, ovarian cancer, and malignant lymphoma [1–7]. Its derivatives are the most clinically used because they bind to type I topoisomerase and inhibit recombination with DNA, inhibiting DNA synthesis, causing cancer cell apoptosis, and resulting in an extremely potent anticancer activity [4]. Irinotecan is biotransformed because of the action of carboxylesterase in SN-38 (7-ethyl-10-hydroxy-20(S)-camptothecin), which lacks a substituent at the 10-position on the piperidine ring. Additionally, the cytotoxicity of SN-38 is 100–1000 times greater than that of irinotecan (Figure S1) [8–10]. However, it causes serious side effects, and there is demand for developing a mechanism such as a drug delivery system (DDS) to deliver specific drugs and reduce dosages [11–16]. For example, a liposomal irinotecan called Onivyde has been reported and approved for medical use [17,18].

Previously, we have reported that thrombin-binding aptamer (TBA) is selectively and efficiently incorporated into the gel through thrombin during the fibrin gel formation known as the blood coagulation reaction [19–24]. In the fibrin gel formation process, first, thrombin cleaves FpA and FpB from the Aα and Bβ chains located at the N-terminus of fibrinogen to produce fibrin monomers [25]. The resulting fibrin monomer engulfs thrombin and polymerizes to form a gel. Therefore, it was suggested that by using this phenomenon named selective oligonucleotide entrapment in fibrin polymers (SOEF), the desired substance or functional group could be introduced into the fibrin gel with TBA [26].

Recently, it has been shown that fibrin plays an important role when cancer cells metastasize or invade other organs, and that fibrinogen is abundant in the cancer stroma [11]. When considering SOEF,

the bifunctional aptamer (bApt), which is a combined 29-mer TBA and camptothecin binding aptamer, can deliver and condense camptothecin as a potent anticancer drug around cancer cells and efficiently suppress their cell growth (Figure 1). Previously, we developed a camptothecin (CPT)-binding modified DNA aptamer (CMA-70), which is a base-modified DNA aptamer obtained by the systematic evolution of ligands via the exponential enrichment (SELEX) method targeting the camptothecin derivative (CPT1) (Figure 1) [27–29]. Therefore, the ability to selectively introduce CPT1 into fibrin gel using bApt as a drug carrier under the SOEF phenomenon provides a new strategy for cancer chemotherapy [30]. However, as a shortcut to the practical application of the said DDS, it is desirable to use an approved anticancer drug such as irinotecan, and thus, this study was conducted.
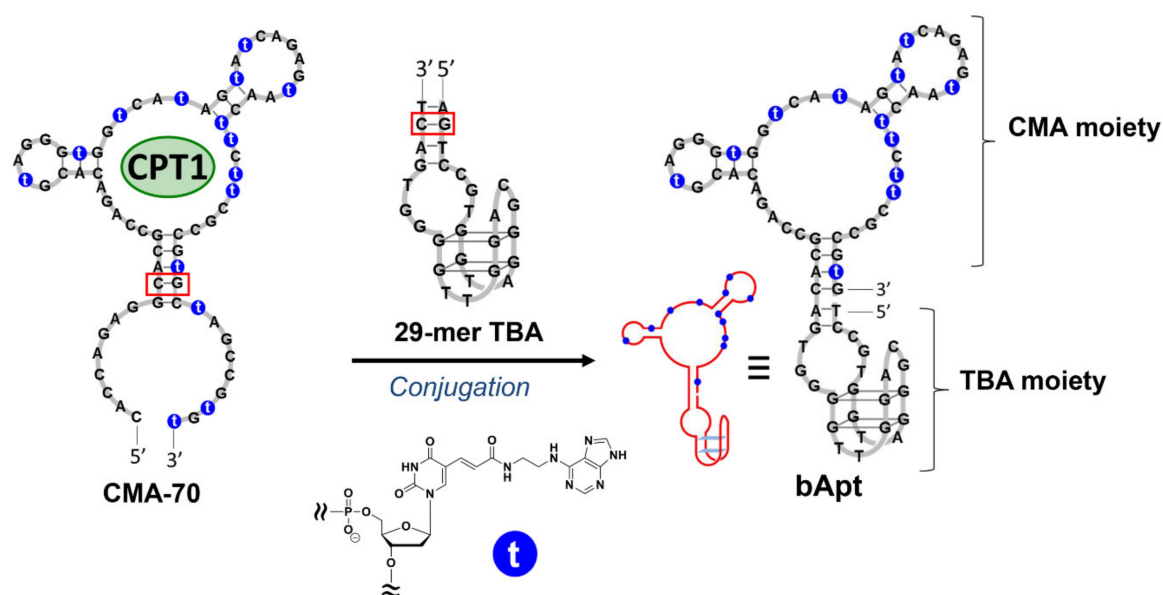

Figure 1. Design of bifunctional aptamer (bApt) conjugated with 29-mer thrombin-binding aptamer (TBA) and a camptothecin (CPT)-binding modified DNA aptamer (CMA-70) containing modified nucleic acids (2'-deoxyuridine-5'-phosphate (dU^{ad}TP)) represented with 't.' Red boxes indicate the conjugation site.

2. Materials and Methods

2.1. Materials

To synthesize CMA-70 and bApt, oligonucleotides, nucleoside triphosphates (dATP, dGTP, dCTP), and *KOD dash* DNA polymerase were, respectively, purchased from Japan Bio Services Co. Ltd. (Saitama, Japan), Roche Diagnostics K. K. (Tokyo, Japan), and Toyobo Co. Ltd. (Tokyo, Japan). For the fluorescence polarization assay, human fibrinogen and thrombin were purchased from Merck K. K. (Tokyo, Japan) and irinotecan and CPT were supplied by Tokyo Chemical Industry Co., Ltd. (Tokyo, Japan). For the cell cultivation and cell growth inhibition assay, Dulbecco's Modified Eagle's Medium (DMEM) low glucose were purchased from Wako Pure Chemical Industries, Ltd., fetal bovine serum (Gibco™) was purchased from Thermo Fischer Scientific K. K. (Tokyo, Japan), CellTracker™ Green CMFDA (5-chloromethylfluorescein diacetate) Dye was purchased from Life Technologies Japan, Ltd. (Osaka, Japan), and HeLa cells (JCRB9004) were purchased from the National Institutes of Biomedical Innovation, Health and Nutrition (Osaka, Japan). All other reagents were of research grade.

2.2. Enzymatic Synthesis of CMA-70 and bApt

The CMA-70 aptamer was synthesized by one-primer PCR using a primer (CMA-70_P1), a template (CMA-70_Temp), three 2'-deoxyribonucleoside triphosphates (dATP, dGTP, and dCTP), and a

modified 2′-deoxyuridine-5′-triphosphate (dU^{ad}TP) with *KOD Dash* DNA polymerase (Table S1) [27,29]. The antisense strand of 5′-monophosphate-labeled ODNs (CMA-70_Temp) was selectively degraded through λ-exonuclease treatment. Then, the resulting CMA-70 was purified via polyacrylamide gel electrophoresis.

The aptamer bApt was synthesized by one-primer PCR using a primer (TBA_P1), a template (T1), three 2′-deoxyribonucleoside triphosphates (dATP, dGTP, and dCTP), and a modified 2′-deoxyuridine-5′-triphosphate (dU^{ad}TP) with *KOD Dash* DNA polymerase (Table S1) [30]. The synthesized bApt was purified by polyacrylamide gel electrophoresis (Figure S2).

2.3. Fluorescence Polarization Assay for CMA-70 Versus CPT Derivatives

To analyze target binding specificity, a fluorescence polarization assay for a target (CPT1, irinotecan, and CPT; final concentration of 0.10 µM) with increasing concentrations of CMA-70 (final concentrations of 0, 0.010, 0.025, 0.050, 0.075, 0.10, 0.50, and 1.0 µM) were performed at 25 °C using an LS-55 fluorescence spectrometer.

First, CMA-70 was dissolved in $1 \times$ phosphate-buffered saline (PBS) (11.8 mM HPO$_4^{2-}$, 140 mM Cl$^-$, 157 mM Na$^+$, 4.5 mM K$^+$; pH 7.4) at appropriate concentrations (2.0 µM), refolded by denaturing at 94 °C for 0.5 min to protect modified nucleic acids and subsequently cooled to 25 °C at a rate of 0.5 °C/min. Each CMA-70 solution (50 µL each) was mixed with 50 µL of a target solution (CPT1, irinotecan and CPT; 0.20 µM) in a PBS buffer, and incubated at 25 °C for 1 h. Fluorescence polarization for each mixture described above was recorded every 20–30 s for 20 min with excitation at 372 nm and monitoring at 456 nm of 25 °C. Thus, fluorescence polarization at 8 aptamer concentrations was generated as curve (Figure 2).

2.4. Fluorescence Polarization Assay for Time Course Analyses of bApt Complexes

Thrombin was dissolved in distilled water, and then, a 2.0 µM thrombin solution in $1 \times$ PBS was prepared. Similarly, mother liquors of fibrinogen (20 µM) and irinotecan (1.0 µM) were prepared in $1 \times$ PBS.

A solution containing bApt (1.0 µM) was prepared in $1 \times$ PBS, and then, bApt was refolded by annealing (preheating at 94 °C for 0.5 min followed by cooling to 25 °C at a rate of 0.5 °C/min). First, the irinotecan solution (63 µL, 1.1 µM) was placed in a 1 cm cuvette and a started fluorescence polarization measurement. After 20 min, the bApt solution (7 µL, 1.0 µM) was put in the same cuvette. Subsequently, the thrombin solution (3.5 µL, 2.0 µM) was added to produce a ternary complex of thrombin, irinotecan, and bApt after 40 min of FP measurement. Finally, fibrinogen solution (3.5 µL, 20 µM) was added after 60 min of FP measurement and measured FP for another 20 min (Figure 3). The final concentration of thrombin/irinotecan/bApt was 0.10 µM and fibrinogen was 1.0 µM.

2.5. Cell Cultivation and Cell Growth Inhibition Assay

Trypsinized HeLa cells were diluted to a concentration of 1.0×10^4 cells/mL with a fresh medium containing DMEM-low glucose, a heat-inactivated serum (Gibco^{TM}, FBS, US origin), and an antibiotic solution (penicillin–streptomycin) at a percentage proportion of 90/9/1 (v/v/v%). The medium (300 µL) containing the cells was transferred to a 96-well tissue culture plate. Then, the cells were cultured in a humidified incubator containing 95% air and 5% CO$_2$ at 37 °C for 24 h. After 240 µL of the medium was removed, 240 µL of the new medium was added to each well. Then, 30 µL of the fibrinogen solution (10 µM) was added and mixed via gentle pipetting. Subsequently, the solution of the ternary thrombin/CPT1/bApt complex (30 µL, 1.0 µM) was added and mixed by gentle pipetting. Solutions of the binary thrombin/TBA complex and free CPT1 (30 µL, 1.0 µM each) were used as controls. Similarly, the abovementioned solutions for the other control experiments were examined. Furthermore, control experiments without fibrinogen (replaced with 1× PBS) were conducted. The cells were cultured in a humidified incubator containing 95% air and 5% CO$_2$ at 37 °C for 48 h.

Next, 300 μL of the medium was replaced with 100 μL of medium containing DMEM-low glucose and CellTracker[TM] Green CMFDA dye in dimethyl sulfoxide (10 mM) at a percentage proportion of 99.8/0.2 (v/v%). The sample was then incubated in a humidified incubator containing 95% air and 5% CO_2 at 37 °C for 30 min. After 300 μL of the medium was replaced with 300 μL of 1× PBS, the stained cell layer was examined under a BZ-X710 inverted fluorescence microscope to acquire fluorescence images (40×) using excitation light (480 nm) and a cut-off filter (<520 nm) (Figure 4). Three independent experiments were performed.

3. Results

3.1. Fluorescence Polarization Assay Using CMA-70

The fluorescence polarization measurement was conducted to examine the binding properties to CPT1, irinotecan, and camptothecin (CPT) (Figure 2A–C) using CMA-70, which is the mother aptamer of the camptothecin-derivative-binding site in bApt. From Figure 2D, we revealed that the fluorescence polarization degree (ΔFP) of irinotecan increases depending on the CMA-70 concentration, as in CPT1 and CPT. It was indicated that the affinity of CMA-70 for irinotecan exceeded that of CPT.
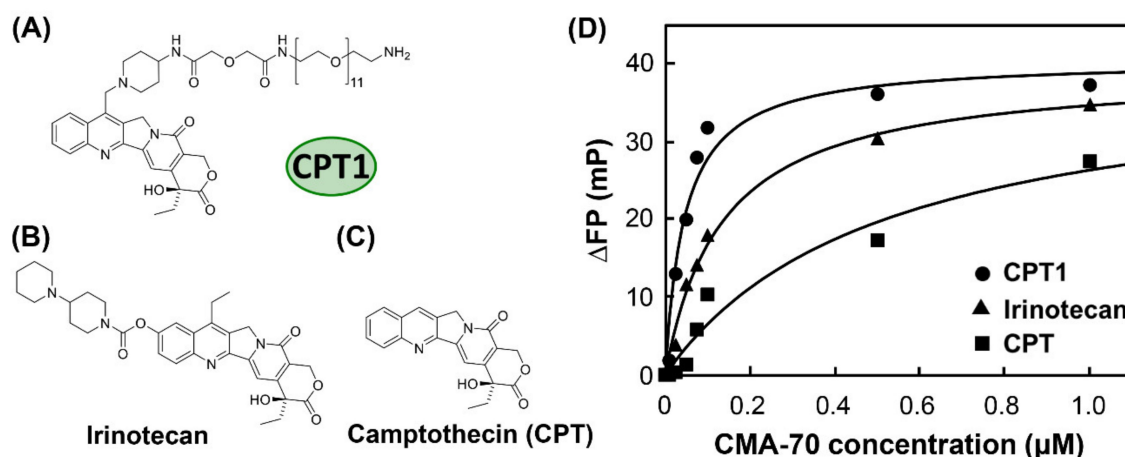

Figure 2. Chemical structures of (**A**) camptothecin derivative (CPT1), (**B**) irinotecan, and (**C**) camptothecin (CPT) and (**D**) titration curves for CPT1 (•), irinotecan (▲), and CPT (■) polarization versus CMA-70 concentration; polarization was monitored at 456 nm using the excitation wavelength of CPT1, irinotecan, and CPT (372 nm).

3.2. Fluorescence Polarization Assay Using bApt

Next, fluorescence polarization measurements of irinotecan were performed to observe the stepwise binding of bApt to its target and the uptake into fibrin gels (Figure 3). Figure 3A shows the time course in differential fluorescence polarization degrees by (i) addition of bApt to irinotecan, (ii) addition of thrombin, and (iii) addition of fibrinogen, followed by polymerization (gelation) of the fibrin monomer generated by thrombin cleavage activity. From Figure 3B, irinotecan bound to the CMA moiety of bApt, as the addition of bApt increased the fluorescence polarization by approximately 4 mP. Furthermore, by adding thrombin, thrombin bound to the TBA moiety of bApt, which increased the fluorescence polarization by approximately 18 mP. Finally, when fibrinogen was added, the fluorescence polarization degree increased by approximately 120 mP, indicating that irinotecan was incorporated into the gel along with bApt during the process of fibrin gel formation.
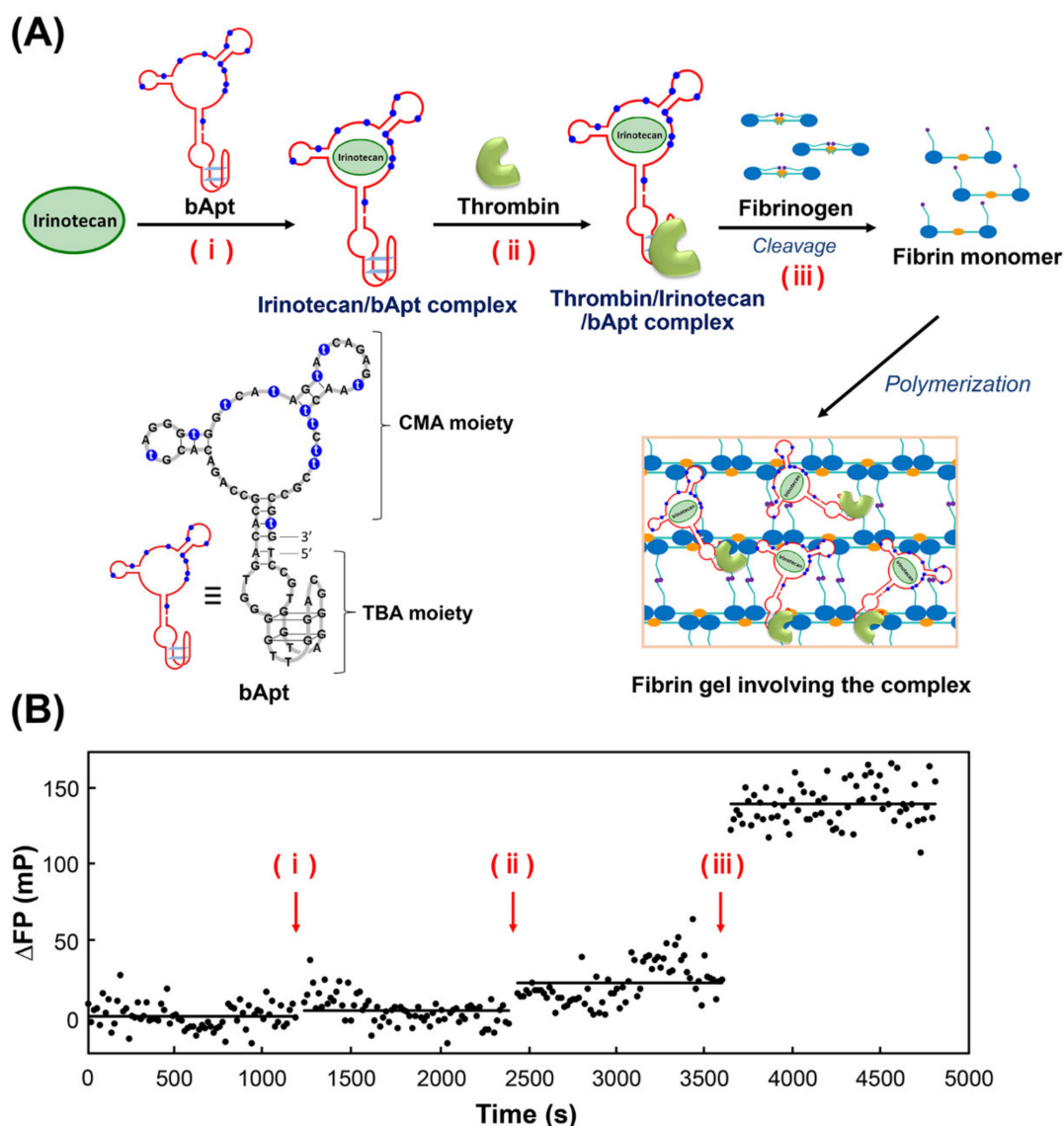
Figure 3. Mechanism of in situ condensation in fibrin gel based on the selective oligonucleotide entrapment in fibrin polymers (SOEF) phenomenon; entrapment of (**A**) the thrombin/irinotecan/bApt complex during the fibrin gel formation. (**B**) The titration curves for irinotecan polarization versus bApt concentration; polarization was monitored at 456 nm using an excitation wavelength of 372 nm.

3.3. Cell Growth Inhibition Assay

Finally, cell growth inhibition assays were performed using HeLa cells to verify whether bApt could be used as a drug carrier for irinotecan. Fluorescent staining uses CellTracker™, which can selectively stain only live cells. From Figure 4D,H, nonemissive images were obtained only in the presence of thrombin/CPT1/bApt complex or thrombin/irinotecan/bApt complex after 48 h incubation. Furthermore, the fibrin gels containing bApt are not cytotoxic [30]. Thus, it was demonstrated that a significant inhibition of cell proliferation occurs in irinotecan and CPT1 under the SOEF phenomenon.
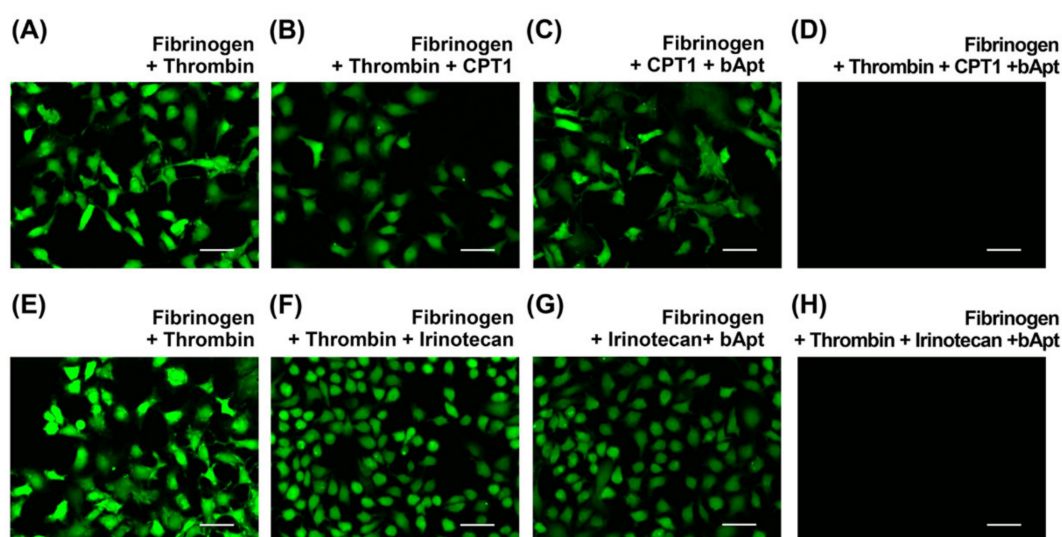
Figure 4. Fluorescence microscopy images of the HeLa cells incubated for 48 h at 37 °C after addition of (**A**,**E**) fibrinogen and thrombin, (**B**,**F**) fibrinogen, thrombin and CPT1 or irinotecan, (**C**,**G**) fibrinogen, CPT1 or irinotecan, and bApt, and (**D**,**H**) fibrinogen, thrombin, CPT1 or irinotecan, and bApt. The thrombin, CPT1 or irinotecan, and bApt concentrations are 100 nM each and fibrinogen concentration is 1000 nM. Scale bar = 50 μm.

4. Discussion

Fluorescence polarization measurements showed that the CMA part of bApt binds to irinotecan, and further, the irinotecan-binding bApt is efficiently incorporated into fibrin gels by binding the TBA part of bApt to thrombin. Furthermore, cell assays revealed that fibrin gels densely containing irinotecan can cause cancer cell death.

In this study, 29-mer TBA was used at the TBA part of bApt known to have a K_d value of 0.5 nM for thrombin. This binding to thrombin can delay the blood coagulation reaction by about 16 s compared to the normal condition without any inhibitors [24]. Meanwhile, in the presence of TBAs with different sequences of similar lengths (15–38 mer) with K_d values of 0.7–126 nM for thrombin, their blood coagulation reactions were delayed by about 2 s [24]. Therefore, the 29-mer TBA sequence used in this study has a relatively high affinity for thrombin and exhibits inhibitory activity although it does not completely inhibit the activity of thrombin.

Currently, phenomena in which thrombin bound to iron oxide nanoparticles is incorporated into fibrin gels were observed with electron microscopes [31]. Those reports agree with the efficient introduction of bApt into fibrin gels due to the high avidity of the TBA to thrombin and the efficient thrombin-mediated uptake of TBA into fibrin gels observed in this study [26,30].

Moreover, in this study, irinotecan was loaded at the CMA site of bApt instead of CPT1. Recently, we have demonstrated that using bApt carrying CPT1, CPT1 was concentrated in a thin layer of about 50 μm thickness formed by fibrin gels, and thereby the growth inhibitory effect on cancer cells appeared more significantly about 182 times higher than that of CPT1 only [30]. The inhibitory concentration (IC_{50}) values of CPT1 entrapped in fibrin gel (7.6 ± 0.36 nM) were approximately 170 times lower than that of CPT1 only in the culture medium (1300 ± 600 nM) [30]. Similarly, in this study, irinotecan was concentrated in a thin layer formed by fibrin gel and assimilated into the cell, resulting in a higher cancer cell growth inhibitory effect when compared with that obtained only using irinotecan. The IC_{50} values of irinotecan for HeLa cell were 1320 ± 130 nM [2,32]. Therefore, the IC_{50} values of irinotecan entrapped in fibrin gel were estimated to be approximately several nM to several tens of nM.

For the application of bifunctional molecular recognition biomolecules to pharmaceuticals, an antibody (emicizumab) with two target recognition sites is currently approved for treating hemophilia [33,34]. Conversely, for using a nucleic acid aptamer, it has been reported that

aptamer–aptamer conjugates enable signal control of tyrosine kinase receptor [35] or delivery of doxorubicin to the tumor cell/brain lesions [36], and aptamer–antibody or aptamer–aptamer conjugate can attract T and cancer cells and destroy cancer cells [37–39]; however, they have not been practically used [35–40].

The bApt oligonucleotide has the activity of binding to both the anticancer drug and thrombin, and acts as a carrier for anticancer drugs, which enables the concentration of the anticancer drug in fibrin gels around growing cancer cells. In the future, in the design of bApt, the anticancer drug binding site is compatible with other functionalities. Therefore, the concept and methodology may also be applicable to diseases related to blood coagulation in the future.

5. Conclusions

We demonstrated that the approved drug irinotecan can be selectively and efficiently concentrated into fibrin gels. In the future, the bApt we have developed can be applied as a drug carrier to DDS of anticancer agents around cancer tissues where fibrin production is active. Furthermore, creating drug carriers using a combination of approved drugs and their aptamers and their application to DDS are expected to be applied to diseases related to fibrin, such as blood coagulation disorders.

Author Contributions: Conceptualization, M.K.; methodology, M.K.; validation, H.F. and Y.K.; formal analysis, H.F. and Y.K.; investigation, H.F. and Y.K.; data curation, H.F. and Y.K.; writing—original draft preparation, H.F. and Y.K.; writing—review and editing, H.F., Y.K. and M.K.; supervision, M.K.; project administration, M.K.; funding acquisition, M.K. All authors have read and agreed to the published version of the manuscript.

Conflicts of Interest: The authors declare no conflict of interest.

References

1. Shetty, D.; Skorjanc, T.; Olson, M.A.; Trabolsi, A. Self-assembly of stimuli-responsive imine-linked calix[4]arene nanocapsules for targeted camptothecin delivery. *Chem. Commun.* **2019**, *55*, 8876–8879. [CrossRef]
2. Zhou, M.; Liu, M.; He, X.; Yu, H.; Wu, D.; Yao, Y.; Fan, S.; Zhang, P.; Shi, W.; Zhong, B. Synthesis and biological evaluation of novel 10-substituted-7-ethyl-10-hydroxycamptothecin (SN-38) prodrugs. *Molecules* **2014**, *19*, 19718–19731. [CrossRef]
3. Li, X.Q.; Wen, H.Y.; Dong, H.Q.; Xue, W.M.; Pauletti, G.M.; Cai, X.J.; Xia, W.J.; Shi, D.; Li, Y.Y. Self-assembling nanomicelles of a novel camptothecin prodrug engineered with a redox-responsive release mechanism. *Chem. Commun.* **2011**, *47*, 8647–8649. [CrossRef] [PubMed]
4. Pommier, Y. Topoisomerase I inhibitors: Camptothecins and beyond. *Nat. Rev. Cancer* **2006**, *6*, 789–802. [CrossRef] [PubMed]
5. Cheng, K.; Rahier, N.J.; Eisenhauer, B.M.; Gao, R.; Thomas, S.J.; Hecht, S.M. 14-Azacamptothecin: A potent water-soluble topoisomerase I poison. *J. Am. Chem. Soc.* **2005**, *127*, 838–839. [CrossRef] [PubMed]
6. Pizzolato, J.F.; Saltz, L.B. The camptothecins. *Lancet* **2003**, *361*, 2235–2242. [CrossRef]
7. Arimondo, P.B.; Boutorine, A.; Baldeyrou, B.; Bailly, C.; Kuwahara, M.; Hecht, S.M.; Sun, J.S.; Garestier, T.; Helene, C. Design and optimization of camptothecin conjugates of triple helix-forming oligonucleotides for sequence-specific DNA cleavage by topoisomerase I. *J. Biol. Chem.* **2002**, *277*, 3132–3140. [CrossRef]
8. Fujita, K.; Kubota, Y.; Ishida, H.; Sasaki, Y. Irinotecan, a key chemotherapeutic drug for metastatic colorectal cancer. *World J. Gastroenterol.* **2015**, *21*, 12234–12248. [CrossRef]
9. Iyer, L.; King, C.D.; Whitington, P.F.; Green, M.D.; Roy, S.K.; Tephly, T.R.; Coffman, B.L.; Ratain, M.J. Genetic predisposition to the metabolism of irinotecan (CPT-11). Role of uridine diphosphate glucuronosyltransferase isoform 1A1 in the glucuronidation of its active metabolite (SN-38) in human liver microsomes. *J. Clin. Investig.* **1998**, *101*, 847–854. [CrossRef]

10. Kunimoto, T.; Nitta, K.; Tanaka, T.; Uehara, N.; Baba, H.; Takeuchi, M.; Yokokura, T.; Sawada, S.; Miyasaka, T.; Mutai, M. Antitumor activity of 7-ethyl-10-[4-(1-piperidino)-1-piperidino]carbonyloxy-camptothec in, a novel water-soluble derivative of camptothecin, against murine tumors. *Cancer Res.* **1987**, *47*, 5944–5947.

11. Gurav, D.; Varghese, O.P.; Hamad, O.A.; Nilsson, B.; Hilborn, J.; Oommen, O.P. Chondroitin sulfate coated gold nanoparticles: A new strategy to resolve multidrug resistance and thromboinflammation. *Chem. Commun.* **2016**, *52*, 966–969. [CrossRef]

12. Li, J.; Mo, L.; Lu, C.H.; Fu, T.; Yang, H.H.; Tan, W. Functional nucleic acid-based hydrogels for bioanalytical and biomedical applications. *Chem. Soc. Rev.* **2016**, *45*, 1410–1431. [CrossRef] [PubMed]

13. Li, H.; Arroyo-Curras, N.; Kang, D.; Ricci, F.; Plaxco, K.W. Dual-reporter drift correction to enhance the performance of electrochemical aptamer-based sensors in whole blood. *J. Am. Chem. Soc.* **2016**, *138*, 15809–15812. [CrossRef] [PubMed]

14. McKeague, M.; De Girolamo, A.; Valenzano, S.; Pascale, M.; Ruscito, A.; Velu, R.; Frost, N.R.; Hill, K.; Smith, M.; McConnell, E.M.; et al. Comprehensive analytical comparison of strategies used for small molecule aptamer evaluation. *Anal. Chem.* **2015**, *87*, 8608–8612. [CrossRef]

15. Coles, D.J.; Rolfe, B.E.; Boase, N.R.; Veedu, R.N.; Thurecht, K.J. Aptamer-targeted hyperbranched polymers: Towards greater specificity for tumours in vivo. *Chem. Commun.* **2013**, *49*, 3836–3838. [CrossRef]

16. Shoji, A.; Kuwahara, M.; Ozaki, H.; Sawai, H. Modified DNA aptamer that binds the (R)-isomer of a thalidomide derivative with high enantioselectivity. *J. Am. Chem. Soc.* **2007**, *129*, 1456–1464. [CrossRef]

17. Koeller, J.; Surinach, A.; Arikian, S.R.; Zivkovic, M.; Janeczko, P.; Cockrum, P.; Kim, G. Comparing real-world evidence among patients with metastatic pancreatic ductal adenocarcinoma treated with liposomal irinotecan. *Ther. Adv. Med. Oncol.* **2020**, *12*, 1–8. [CrossRef]

18. Kciuk, M.; Marciniak, B.; Kontek, R. Irinotecan-Still an Important Player in Cancer Chemotherapy: A Comprehensive Overview. *Int. J. Mol. Sci.* **2020**, *21*, 4919. [CrossRef] [PubMed]

19. Riccardi, C.; Napolitano, E.; Platella, C.; Musumeci, D.; Montesarchio, D. G-quadruplex-based aptamers targeting human thrombin: Discovery, chemical modifications and antithrombotic effects. *Pharmacol. Ther* **2020**, 107649, in press. [CrossRef] [PubMed]

20. Chabata, C.V.; Frederiksen, J.W.; Sullenger, B.A.; Gunaratne, R. Emerging applications of aptamers for anticoagulation and hemostasis. *Curr. Opin. Hematol.* **2018**, *25*, 382–388. [CrossRef] [PubMed]

21. Takahashi, S.; Sugimoto, N. Volumetric contributions of loop regions of G-quadruplex DNA to the formation of the tertiary structure. *Biophys. Chem.* **2017**, *231*, 146–154. [CrossRef] [PubMed]

22. Kasahara, Y.; Irisawa, Y.; Fujita, H.; Yahara, A.; Ozaki, H.; Obika, S.; Kuwahara, M. Capillary electrophoresis-systematic evolution of ligands by exponential enrichment selection of base- and sugar-modified DNA aptamers: Target binding dominated by 2′-O,4′-C-methylene-bridged/locked nucleic acid primer. *Anal. Chem.* **2013**, *85*, 4961–4967. [CrossRef] [PubMed]

23. Kasahara, Y.; Irisawa, Y.; Ozaki, H.; Obika, S.; Kuwahara, M. 2′,4′-BNA/LNA aptamers: CE-SELEX using a DNA-based library of full-length 2′-O,4′-C-methylene-bridged/linked bicyclic ribonucleotides. *Bioorg. Med. Chem. Lett.* **2013**, *23*, 1288–1292. [CrossRef] [PubMed]

24. Tasset, D.M.; Kubik, M.F.; Steiner, W. Oligonucleotide inhibitors of human thrombin that bind distinct epitopes. *J. Mol. Biol.* **1997**, *272*, 688–698. [CrossRef]

25. Mosesson, M.W. Fibrinogen and fibrin structure and functions. *J. Thromb. Haemost.* **2005**, *3*, 1894–1904. [CrossRef]

26. Fujita, H.; Inoue, Y.; Kuwahara, M. Selective incorporation of foreign functionality into fibrin gels through a chemically modified DNA aptamer. *Bioorg. Med. Chem. Lett.* **2018**, *28*, 35–39. [CrossRef]

27. Fujita, H.; Kuwahara, M. Selection of Natural and Base-Modified DNA Aptamers for a Camptothecin Derivative. *Curr. Protoc. Nucleic Acid Chem.* **2016**, *65*, 9.10.1–9.10.19. [CrossRef]

28. Fujita, H.; Imaizumi, Y.; Kasahara, Y.; Kitadume, S.; Ozaki, H.; Kuwahara, M.; Sugimoto, N. Structural and affinity analyses of g-quadruplex DNA aptamers for camptothecin derivatives. *Pharmaceuticals* **2013**, *6*, 1082–1093. [CrossRef]

29. Imaizumi, Y.; Kasahara, Y.; Fujita, H.; Kitadume, S.; Ozaki, H.; Endoh, T.; Kuwahara, M.; Sugimoto, N. Efficacy of base-modification on target binding of small molecule DNA aptamers. *J. Am. Chem. Soc.* **2013**, *135*, 9412–9419. [CrossRef]

30. Kuwahara, M.; Fujita, H.; Kataoka, Y.; Nakajima, Y.; Yamada, M.; Sugimoto, N. In situ condensation of an anti-cancer drug into fibrin gel enabling effective inhibition of tumor cell growth. *Chem. Commun.* **2019**, *55*, 11679–11682. [CrossRef]

31. Ziv-Polat, O.; Skaat, H.; Shahar, A.; Margel, S. Novel magnetic fibrin hydrogel scaffolds containing thrombin and growth factors conjugated iron oxide nanoparticles for tissue engineering. *Int. J. Nanomed.* **2012**, *7*, 1259–1274. [CrossRef]

32. Takara, K.; Kitada, N.; Yoshikawa, E.; Yamamoto, K.; Horibe, S.; Sakaeda, T.; Nishiguchi, K.; Ohnishi, N.; Yokoyama, T. Molecular changes to HeLa cells on continuous exposure to SN-38, an active metabolite of irinotecan hydrochloride. *Cancer Lett.* **2009**, *278*, 88–96. [CrossRef] [PubMed]

33. Kitazawa, T.; Shima, M. Emicizumab, a humanized bispecific antibody to coagulation factors IXa and X with a factor VIIIa-cofactor activity. *Int. J. Hematol.* **2020**, *111*, 20–30. [CrossRef] [PubMed]

34. Sampei, Z.; Igawa, T.; Soeda, T.; Okuyama-Nishida, Y.; Moriyama, C.; Wakabayashi, T.; Tanaka, E.; Muto, A.; Kojima, T.; Kitazawa, T.; et al. Identification and multidimensional optimization of an asymmetric bispecific IgG antibody mimicking the function of factor VIII cofactor activity. *PLoS ONE* **2013**, *8*, e57479. [CrossRef] [PubMed]

35. Ueki, R.; Atsuta, S.; Ueki, A.; Sando, S. Nongenetic Reprogramming of the Ligand Specificity of Growth Factor Receptors by Bispecific DNA Aptamers. *J. Am. Chem. Soc.* **2017**, *139*, 6554–6557. [CrossRef] [PubMed]

36. Macdonald, J.; Denoyer, D.; Henri, J.; Jamieson, A.; Burvenich, I.J.G.; Pouliot, N.; Shigdar, S. Bifunctional Aptamer-Doxorubicin Conjugate Crosses the Blood-Brain Barrier and Selectively Delivers Its Payload to EpCAM-Positive Tumor Cells. *Nucleic Acid Ther.* **2020**, *30*, 117–128. [CrossRef]

37. Yang, Y.; Sun, X.; Xu, J.; Cui, C.; Safari Yazd, H.; Pan, X.; Zhu, Y.; Chen, X.; Li, X.; Li, J.; et al. Circular Bispecific Aptamer-Mediated Artificial Intercellular Recognition for Targeted T Cell Immunotherapy. *ACS Nano* **2020**, *14*, 9562–9571. [CrossRef]

38. Passariello, M.; Camorani, S.; Vetrei, C.; Cerchia, L.; De Lorenzo, C. Novel Human Bispecific Aptamer-Antibody Conjugates for Efficient Cancer Cell Killing. *Cancers* **2019**, *11*, 1268. [CrossRef]

39. Boltz, A.; Piater, B.; Toleikis, L.; Guenther, R.; Kolmar, H.; Hock, B. Bi-specific aptamers mediating tumor cell lysis. *J. Biol. Chem.* **2011**, *286*, 21896–21905. [CrossRef]

40. Riccardi, C.; Napolitano, E.; Musumeci, D.; Montesarchio, D. Dimeric and Multimeric DNA Aptamers for Highly Effective Protein Recognition. *Molecules* **2020**, *25*, 5227. [CrossRef]